Time-reversal violating Schiff moment of [225]Ra

J. Engel,[1,*] M. Bender,[2,†] J. Dobaczewski,[3,‡] J. H. de Jesus,[1,§] and P. Olbratowski[3,4,‖]

[1]*Department of Physics and Astronomy, CB3255, University of North Carolina, Chapel Hill, North Carolina 27599-3255, USA*

[2]*Service de Physique Nucléaire Théorique et de Physique Mathématique, Université Libre de Bruxelles—Case Postale 229, B-1050 Brussels, Belgium*

[3]*Institute of Theoretical Physics, Warsaw University, Hoża 69, PL-00681 Warsaw, Poland*

[4]*Institut de Recherches Subatomiques, UMR7500, CNRS-IN2P3 and Université Louis Pasteur, F-67037 Strasbourg Cedex 2, France*

We use the Skyrme-Hartree-Fock method, allowing all symmetries to be broken, to calculate the time-reversal-violating nuclear Schiff moment (which induces atomic electric dipole moments) in the octupole-deformed nucleus [225]Ra. Our calculation includes several effects neglected in an earlier work, including self-consistency and polarization of the core by the last nucleon. We confirm that the Schiff moment is large compared to those of reflection-symmetric nuclei, though ours is generally a few times smaller than recent estimates.

I. INTRODUCTION

Experiments with K and B mesons indicate that time-reversal invariance (T) is violated through phases in the Cabibbo-Kobayashi-Maskawa matrix that affect weak interactions [1]. The suspicion that extra-standard-model physics, e.g., supersymmetry, also violates T has motivated a different kind of experiment: measuring the electric dipole moments (EDMs) of the neutron and atoms. Because any such dipole moment must be proportional to the expectation value of the T-odd spin operator, it can only exist when T (and parity, P) is violated [2,3]. So far the experiments have measured no dipole moments, but they continue to improve and even null results are useful, since they seriously constrain new physics. Whatever the experimental situation in the future, therefore, it is important to determine theoretically what the presence or absence of EDMs at a given level implies about T-violating interactions at elementary-particle scales. Our focus here is on atoms, which for some sources of T violation currently provide limits as good or better than the neutron [4].

One way an atom can develop an EDM is through T and P violation in its nucleus. Let us assume that given a fundamental source of the broken symmetry, one can use effective-field theory and QCD to calculate the strength of the resulting T-violating nucleon-pion interaction. One then needs to connect the strength of that interaction to the resulting nuclear "Schiff moment," which, because the nuclear EDM is screened [5], is the quantity responsible for inducing an EDM in electrons orbiting the nucleus. The Schiff moment is defined classically as a kind of radially weighted dipole moment:

$$S = \frac{1}{10} \int d^3r \, \rho_{ch}(\mathbf{r}) \left(r^2 - \frac{5}{3} \overline{r_{ch}^2} \right) \mathbf{r}, \qquad (1)$$

where ρ_{ch} is the nuclear charge density and $\overline{r_{ch}^2}$ is the mean-square charge radius. Recent papers [6,7] have argued that because of their asymmetric shapes, octupole-deformed nuclei in the light-actinide region should have collective Schiff moments that are 100–1000 times larger than the Schiff moment in [199]Hg, the system with the best experimental limit on its atomic EDM [4]. Reference [8] suggested that certain many-body effects may make the enhancement a bit less than that. The degree of enhancement is important because several experiments in the light actinides are contemplated, planned, or underway [9,10]. Even if they do not see EDM's we will need to know how their limits on T-violation compared with limits from other experiments.

Perhaps the most interesting octupole-deformed nucleus for an experiment is [225]Ra. Though radioactive, it has a ground-state angular momentum $J = 1/2$, which minimizes the effect of stray quadrupole electric fields in an experiment to measure a dipole moment.[1] In addition, the associated atom has close-lying electronic levels of opposite parity and is relatively easy to trap and manipulate. As a result, at least one group is at work on a measurement in [225]Ra [10]. Here, we calculate its Schiff moment, attempting to incorporate the effects discussed in Ref. [8] through a symmetry-unrestricted mean-field calculation. We begin the following section by describing the physics of the Schiff moment in octupole-deformed nuclei, briefly reviewing prior work in the process. In Sec. III, we test our mean-field approach by calculating properties of even Ra isotopes. In Sec. IV, we discuss issues peculiar to mean-field calculations in odd nuclei and then present our results for the Schiff moment of [225]Ra, focusing

---

*Email address: engelj@physics.unc.edu

†Email address: mbender@ulb.ac.be

‡Email address: Jacek.Dobaczewski@fuw.edu.pl

§Email address: jhjesus@physics.unc.edu

‖Email address: Przemyslaw.Olbratowski@fuw.edu.pl

---

[1]The statement that the nucleus has octupole and quadrupole deformation really refers to its *intrinsic* state, a concept we elaborate on below, and does not contradict its insensitivity to applied electric fields with multipolarity greater than one.

particularly on the degree of enhancement. Section V is a brief conclusion.

II. ENHANCEMENT OF SCHIFF MOMENTS IN OCTUPOLE-DEFORMED NUCLEI—PREVIOUS WORK

In analogy with dipole moments in atoms, static Schiff moments in nuclei can exist only if T is broken. Because T-violating forces are much weaker than the strong interaction, the Schiff moment can be accurately evaluated through the first-order perturbation theory as

$$S \equiv \langle \Psi_0 | \hat{S}_z | \Psi_0 \rangle = \sum_{i \neq 0} \frac{\langle \Psi_0 | \hat{S}_z | \Psi_i \rangle \langle \Psi_i | \hat{V}_{PT} | \Psi_0 \rangle}{E_0 - E_i} + \text{c.c.},$$
(2)

where $|\Psi_0\rangle$ is the member of the ground-state multiplet with $J_z = J \neq 0$, the sum is over excited states, and $\hat{S}_z$ is the operator,

$$\hat{S}_z = \frac{e}{10} \sum_p \left(r_p^2 - \frac{5}{3} \overline{r_{\text{ch}}^2} \right) z_p,$$
(3)

with the sum here over protons. The operator $\hat{V}_{PT}$ is the T-(and parity-) violating nucleon-nucleon interaction mediated by the pion [11,12] (shown to be more important than other mesons in Ref. [13]):

$$
\hat{V}_{PT}(\boldsymbol{r}_1 - \boldsymbol{r}_2) = -\frac{g\, m_\pi^2}{8\,\pi m_N} \Bigg\{ (\boldsymbol{\sigma}_1 - \boldsymbol{\sigma}_2) \cdot (\boldsymbol{r}_1 - \boldsymbol{r}_2) \Bigg[\bar{g}_0 \vec{\tau}_1 \cdot \vec{\tau}_2
$$
$$
- \frac{\bar{g}_1}{2}(\tau_{1z} + \tau_{2z}) + \bar{g}_2 (3\tau_{1z}\tau_{2z} - \vec{\tau}_1 \cdot \vec{\tau}_2) \Bigg]
$$
$$
- \frac{\bar{g}_1}{2}(\boldsymbol{\sigma}_1 + \boldsymbol{\sigma}_2) \cdot (\boldsymbol{r}_1 - \boldsymbol{r}_2)(\tau_{1z} - \tau_{2z}) \Bigg\}
$$
$$
\times \frac{\exp(-m_\pi |\boldsymbol{r}_1 - \boldsymbol{r}_2|)}{m_\pi |\boldsymbol{r}_1 - \boldsymbol{r}_2|^2} \Bigg[1 + \frac{1}{m_\pi |\boldsymbol{r}_1 - \boldsymbol{r}_2|} \Bigg],
$$
(4)

where arrows denote isovector operators, τ_z is $+1$ for neutrons, m_N is the nucleon mass, and we are using the convention $\hbar = c = 1$. The $\bar{g}$'s are the unknown isoscalar, isovector, and isotensor T-violating pion-nucleon couplings, and g is the usual strong πNN coupling.

In a nucleus such as ^{199}Hg, with no intrinsic octupole deformation, many intermediate states contribute to the sum in Eq. (2). By contrast, the asymmetric shape of ^{225}Ra implies the existence of a very low-energy $|1/2^-\rangle$ state, in this case 55 keV above the ground state $|\Psi_0\rangle \equiv |1/2^+\rangle$, that dominates the sum because of the corresponding small denominator. To a very good approximation, then,

$$S \equiv -\frac{\langle 1/2^+ | \hat{S}_z | 1/2^- \rangle \langle 1/2^- | \hat{V}_{PT} | 1/2^+ \rangle}{\Delta E} + \text{c.c.},$$
(5)

where $\Delta E = 55$ keV. The small denominator is part of the reason for the enhancement of the Schiff moment. The other part is the matrix element of the Schiff operator in Eq. (5). In the limit that the deformation is rigid, the ground state and first excited state in octupole-deformed nuclei are partners in a parity doublet, i.e., projections onto good parity and angular momentum of the same "intrinsic state" that represents the wave function of the nucleus in its own body-fixed frame. The matrix elements in Eq. (5) are then proportional (again, in the limit of rigid deformation) to intrinsic-state expectation values, so that [6]

$$S \rightarrow -2 \frac{J}{J+1} \frac{\langle \hat{S}_z \rangle \langle \hat{V}_{PT} \rangle}{\Delta E},$$
(6)

where J is the ground-state angular momentum, equal to 1/2 for ^{225}Ra, and the brackets indicate expectation values in the intrinsic state. The intrinsic-state expectation value $\langle \hat{S}_z \rangle$ is generated by the collective quadrupole and octupole deformation of the entire nucleus; it is much larger than a typical matrix element in a spherical or symmetrically deformed nucleus. Together with the small energy denominator, this large matrix element is responsible for the enhancement of laboratory-frame Schiff moments in nuclei such as ^{225}Ra.

The amount of enhancement is not easy to calculate accurately, however. The reason is that the matrix element of the two-body spin-dependent operator $\hat{V}_{PT}$ in Eq. (5) depends sensitively on the behavior of a few valence particles, which carry most of the spin. In the approximation that particles (or quasiparticles) move in independent orbits generated by a mean field, the potential can be written as an effective density-dependent one-body operator that we will denote as $\hat{U}_{PT}$, defined implicitly by

$$\langle a | \hat{U}_{PT} | b \rangle = \sum_{c < F} \langle ac | \hat{V}_{PT} | bc \rangle,$$
(7)

where $|a\rangle$, $|b\rangle$, and $|c\rangle$ are eigenstates of the mean field and the matrix elements of $\hat{V}_{PT}$ are antisymmetrized. With the further approximation that the mass of the pion is very large, $\hat{U}_{PT}$ can be written as a local operator, in a form we display in Sec. IV. Evaluation of its matrix element is tricky.

The authors of Refs. [6,7] used a version of the particle-rotor model [14] to represent the odd-A nucleus. In this model, all but one of the nucleons are treated as a rigid core, and the last valence nucleon occupies a deformed single-particle orbit, obtained by solving a Schrödinger equation for a Nilsson or deformed Woods-Saxon potential. The model implies that the core carries no intrinsic spin whatever, that the neutron and proton densities are proportional, and that the exchange terms on the right-hand side of Eq. (7) are negligible. Under these assumptions, $\hat{U}_{PT}$, which now acts only on the single valence nucleon, reduces to [15]

$$\hat{U}_{PT}(\boldsymbol{r}) \approx \eta \frac{G}{2m_N\sqrt{2}} \boldsymbol{\sigma} \cdot \boldsymbol{\nabla} \rho_0(\boldsymbol{r}),$$
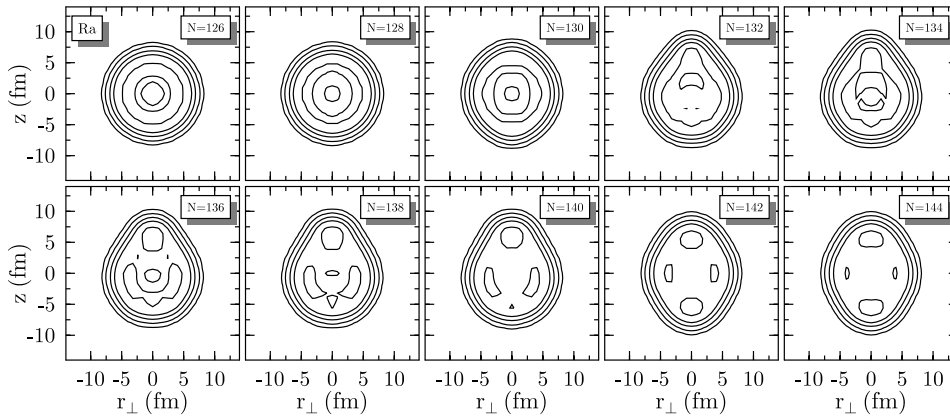(8)

FIG. 1. Contours of constant density for a series of even-N radium isotopes. Contour lines are drawn for densities $\rho = 0.01$, 0.03, 0.07, 0.11, and 0.15 fm^{-3}.

where G is the Fermi constant, inserted to follow convention, and ρ_0 is the total nuclear mass density. The dimensionless parameter η is then a function of the couplings $\bar{g}_i$ and the isospin of the nucleus.

Reference [8] confirmed the collectivity of the intrinsic Schiff moments obtained in Refs. [6,7], but questioned the accuracy of some of the assumptions used to evaluate the matrix element of $\hat{V}_{PT}$, suggesting that either core-spin polarization or self-consistency in the nuclear wave function might reduce laboratory Schiff moments. The zero-range approximation and the neglect of exchange in $\hat{U}_{PT}$ are also open to question. As a result, it is not clear whether the Schiff moment of ^{225}Ra is 1000 times that of ^{199}Hg or 100 times, or even less. In what follows, we provide an (tentative) answer by moving beyond the particle-rotor model. Our calculation is not the final word on Schiff moments in octupole-deformed nuclei—we only consider mean-field theory, neglecting in particular projection onto states with good parity, and do not fully account for the pion's nonzero range — but is a major step forward.

III. MEAN-FIELD CALCULATIONS FOR OTHER Ra ISOTOPES

A. Mean-field calculations

Self-consistent mean-field theory is widely used for describing bulk properties of nuclei [16]. In the guise of density-functional theory, it is also used throughout atomic and molecular physics. The approach is more "microscopic" — nucleons are the only degrees of freedom — and far less phenomenological than the collective particle-rotor model. Self-consistency connects the single-particle states and the actual density distribution. The variational principle that determines the single-particle wave functions thus optimizes all multipole moments not fixed by global symmetries. The density distributions of neutrons and protons are not proportional to each other; they have slightly different deformations and radial profiles. In odd-A nuclei, self-consistent calculations include rearrangement due to the unpaired particle. Rearrangement causes polarization of the even-A core through orbital-current and spin-density terms in the effective interaction. Core polarization is one of the effects on the Schiff moment of ^{225}Ra which we investigate below.

Our approach is nonrelativistic and employs Skyrme interactions. To get an idea of the range of results this kind of calculation can produce, we use four different parametrizations of the Skyrme energy functional, i.e., four different Skyrme forces. These four parametrizations give similar results for many observables near stability, but still have significant differences. Our favorite interaction, for reasons explained below, is SkO$'$ [17,18], but we also show results for the commonly used forces SIII [19], SkM* [20], and SLy4 [21].

B. Related observables in even isotopes

Intrinsic-parity breaking in even radium isotopes is the subject of several theoretical analyses; see the review in Ref. [22] and the more recent studies in Refs. [23,24]. To assess the ability of the Skyrme interactions to handle it, we perform a series of Hartree-Fock (HF) + BCS calculations for even radium isotopes. We use the Skyrme-HF+BCS code from Ref. [25]; it represents single-particle wave functions on an axially symmetric mesh, and uses Fourier definitions of the derivative, $1/r_{\perp}$, and $1/r_{\perp}^2$ operators. We choose 75 grid points in the z direction and 27 in the $r_{\perp}$ (perpendicular) direction, with 0.8 fm between them. The code uses a density-independent zero-range pairing interaction with a self-adjusting cutoff as described in Ref. [26]. For each Skyrme force we adjust the pairing strength separately for protons and neutrons [26]. We should note that other self-consistent mean-field models, namely, HF+BCS with the nonrelativistic Gogny force [27] and the relativistic mean-field model [28], yield results that are similar to those we describe now.

Figure 1 illustrates the calculated evolution of intrinsic deformation with increasing neutron number in the radium isotopes. It shows a plot of the intrinsic ground-state mass-density contours predicted by SkO$'$. The mean-field ground states go from having a spherical shape at the magic number $N=126$ to a quadrupole-deformed (reflection-symmetric) shape at $N=130$, then to quadrupole- +octupole-deformed (reflection-asymmetric) shapes for $132 \lesssim N \lesssim 140$, and finally back to quadrupole-deformed shapes at higher N. Because the ground states are obtained from a variational principle, all shape moments higher than octupole are also optimized (the isoscalar dipole moment is constrained to be zero). The
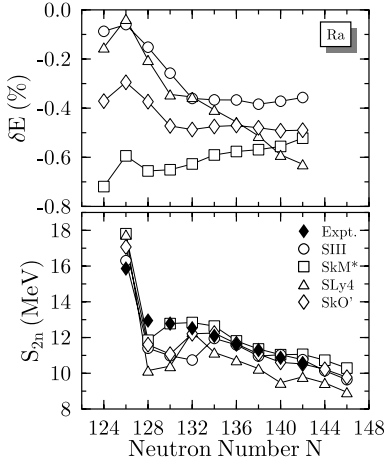
FIG. 2. Relative error in binding energy (top) and predicted two-neutron separation energies (bottom) for four Skyrme interactions in a series of even-*N* radium isotopes. The experimental separation energies are also shown.
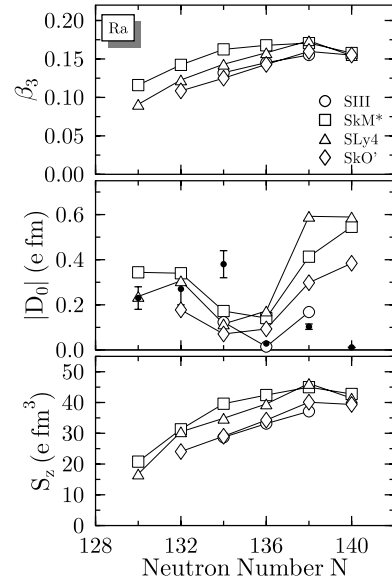

FIG. 3. The predicted first-order [29] octupole deformations (top), intrinsic dipole moments (middle) and intrinsic Schiff moments (bottom) for four Skyrme interactions in a series of even-*N* Radium isotopes. The experimental intrinsic dipole moments are also shown. Where symbols are missing, the corresponding predicted values are zero because the mean field is not asymmetrically deformed.

nucleus ^{225}Ra, with $N=137$, will clearly be well deformed in both quadrupole and octupole coordinates. The structures at small radii visible for $N \geqslant 132$ reflect small oscillations of the density distribution around the saturation value (for a given neutron excess) caused by shell effects.

We must note that the octupole-deformed minima are not equally pronounced for all forces and isotopes. In addition, in some of the isotopes with reflection-symmetric minima, some of the Skyrme forces predict an excited octupole-deformed minimum separated by a small barrier from the ground-state minimum. Furthermore, in the transitional nuclei, which have soft potentials in the octupole direction, all parity-breaking intrinsic deformations are subject to collective correlations as discussed in Ref. [27]. The influence of correlations will be the smallest for the nuclides with the most pronounced octupole-deformed minima, usually ^{222}Ra and ^{224}Ra. This fact supports our belief that our mean-field calculations supply a good approximation to the intrinsic structure in ^{225}Ra.

Figure 2 shows the relative error in the predicted binding energies $\delta E = (E_{\text{calc}} - E_{\text{expt}})/E_{\text{expt}}$ for all four forces, and the predicted two-neutron separation energies, along with the measured values. All the forces do a good job with binding, which is not surprising given the way their parameters were fit. The fact that the error in binding for SkO$'$ is nearly constant with N for $N>130$ is reflected in the near perfect agreement in the bottom panel with the measured two-neutron separation energies S_{2n}. The errors in predicted values of S_{2n} around $N=128$ probably reflect the deficiencies of mean-field models in transitional nuclei.

Figure 3 shows three parity-violating intrinsic quantities. In the top panel is the ground-state octupole deformation $\beta_3 = 4\pi\langle r^3 Y_{30}\rangle/(3AR^3)$ (where $R = 1.2A^{1/3}$) as a function of neutron number. The trend mirrors this in the density profiles shown earlier. At $N=136$, one less neutron than in ^{225}Ra, all the forces predict almost identical octupole deformation, a result we like. Experimental data for octupole moments are still sparse in this region; we are only aware of β_3

$=0.105(4)$ for $N=138$, a value that can be deduced from the $B(E3;0_1^+\rightarrow 3_1^-)$ given in Ref. [30]. (In ^{224}Ra and ^{226}Ra, by the way, we agree fairly well with the quadrupole moments obtained from $B(E2)$'s in Ref. [31]. For example, SkO$'$ gives $\beta_2 = 0.184$ in ^{224}Ra and experiment gives $\beta_2 = 0.179(4)$.)

The second panel in the figure shows the absolute values of intrinsic dipole moments $D_0 = e\Sigma_p\langle z_p\rangle$, along with experimental data extracted from $E1$ transition probabilities [22]. The calculated values for D_0 change sign from positive to negative between $N=134$ and $N=138$, reflecting a small change in the location of the center of charge from the "top" half of the pear-shaped nucleus to the "bottom" half. This predicted sign change is consistent with the near-zero experimental value for $N=136$. None of the forces precisely reproduces the trend through all the isotopes, but the comparison has to be taken with a grain of salt because "data" derive from transitions between excited rotational states and, therefore, are not necessarily identical to the ground-state dipole moments. Cranked Skyrme-HF calculations without pairing correlations [24] and cranked HFB calculations with the Gogny force [23] predict that for most Ra isotopes D_0 changes significantly with angular momentum. In any event, as thoroughly discussed in Ref. [22], the intrinsic dipole moment is a small and delicate quantity.

The intrinsic Schiff moment $\langle S_z \rangle$, the quantity we are really interested in, is more collective and under better control, as the bottom panel of the figure shows. The various predictions are usually within 20% of one another and large, confirming the predictions originally made in Refs. [6,7]. The octupole deformation and intrinsic dipole moment have been shown to change only slightly with parity projection
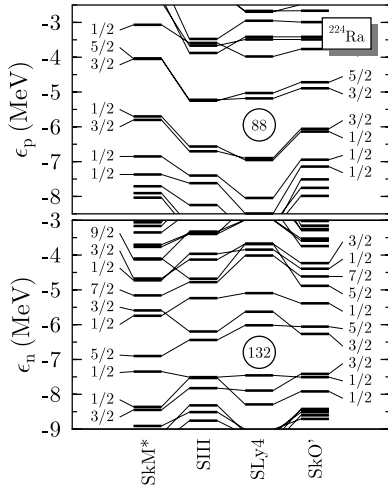
FIG. 4. Single-particle spectra for protons (top) and neutrons (bottom) in ^{224}Ra for the four Skyrme interactions.

from the intrinsic states [23], and the same is probably true of the intrinsic Schiff moment.

By turning the pairing force off, we are able to see whether the parity-violating quantities in Fig. 3 are affected by pairing correlations. In ^{224}Ra, for example, SkO$'$ gives $\beta_3 = 0.141$, $D_0 = -0.103$ e fm, and $\langle S_z \rangle = 34.4$ e fm^3 without pairing, and $\beta_3 = 0.143$, $D_0 = -0.093$ e fm, and $\langle S_z \rangle = 34.3$ e fm^3 when pairing is included. In this nucleus uncertainties related to pairing are very small.

Finally, in Fig. 4, we show the predicted proton and neutron single-particle spectra generated by the ground-state mean-field in ^{224}Ra. The combination of quadrupole, octupole, and higher deformations reduces the level density around the Fermi surface for both kinds of nucleon, leading to significant deformed $Z = 88$ and $N = 132$ shell closures for all interactions, and a somewhat weaker $N = 136$ subshell closure for SIII, SkM*, and SkO$'$. The small level density around the Fermi surface might explain the insensitivity of the deformation to pairing correlations mentioned above. For all the forces except SkM*, the first empty neutron level clearly has $j_z = 1/2$, implying that in ^{225}Ra the ground-state parity-doublet bands will be built on $J^\pi = (1/2)^\pm$ states. For SkM*, the situation is less clear because the $j_z = 1/2$ and $3/2$ states are nearly degenerate, and it is necessary to carry out the calculation in ^{225}Ra itself to see which becomes the lowest.

IV. CALCULATING THE SCHIFF MOMENT OF ^{225}Ra

A. Odd-A nuclei and Schiff moments in mean-field approximation

Fully self-consistent calculations in odd-A nuclei are possible, but seldom performed. For many physical observables it is enough to neglect correlations between the odd particle and the core, which amounts to dropping a valence particle into the field generated by that core. Other quantities, however, are sensitive to the interaction between the last particle and the core. The interaction can change the deformation and the pairing strength, and produce various kinds of core po-

larization. In fact, a self-consistent odd-A calculation is equivalent to first performing the calculation in the even-even nucleus with one less neutron, and then placing the last nucleon in the first empty orbit and treating its polarizing effect on the core in random-phase approximation [32,33]. Fully self-consistent calculations take all kinds of polarization into account simultaneously. For us, the spin polarization is of particular interest.

To proceed here we use the public-domain Skyrme-Hartree-Fock code HFODD (v2.04b) [34–36], which allows the mean-field and the associated Slater determinant to simultaneously break invariance under rotation, reflection through three planes, and time reversal (the code we used in the last section does not). Breaking the first is necessary to describe a deformed nucleus. Breaking all the three reflections (and not only parity) is necessary to represent axial octupole deformation with the spin aligned along the symmetry axis. Breaking the last induces spin polarization in the core, which because of Kramers degeneracy cannot otherwise occur. Incorporating spin polarization is important because it has the potential to significantly alter the matrix element of $\hat{U}_{PT}$ in Eq. (8) from its value in the particle-rotor model, where the spin is carried entirely by one valence particle. The code HFODD cannot yet treat pairing when it allows T to be broken, but pairing in T-odd channels is poorly understood. No existing codes can do more than HFODD in odd-A octupole-deformed nuclei.

As stated above, we use the Skyrme interactions SIII, SkM*, SLy4, and SkO$'$. The reason SkO$'$ is our favorite has to do with the part of the energy functional composed of T-odd spin densities (which, following common practice, we refer to as the "T-odd functional," even though the entire functional must be even under T). The T-odd functional plays no role in the mean-field ground states of even nuclei, but can be important in any state with nonzero angular momentum. Of the forces above, only SkO$'$ has been seriously investigated in T-odd channels. In Ref. [17], the T-odd part of the functional was adjusted to reproduce Gamow-Teller resonances, resulting in an effective Landau parameter g_0' $= 1.2$. In the isoscalar channel, the force was adjusted to reproduce the commonly used value $g_0 = 0.4$ [37]. Although there are not enough data to constrain other relevant parameters in the functional, and although a very recent calculation starting from a realistic nucleon-nucleon interaction [38], while confirming the value $g_0' = 1.2$, finds $g_0 = 0.85$, SkO$'$ is clearly the best available Skyrme interaction for describing spin-spin interactions. The corresponding T-odd terms in the functional are precisely those that will polarize the spin in the core. There are other terms that could be added to the standard Skyrme interaction and do the same thing—the tensor force, for example—but they are almost never used and their effects still need to be investigated.

The parameters of the other three forces SIII, SkM*, and SLy4 were adjusted entirely to ground-state properties in even-even nuclei, and so the Landau parameters g_0 and g_0' were not fit. Here, we set them to zero by treating the T-odd and T-even terms in the Skyrme functional independently, as described in Ref. [17]. Only orbital terms, which are fixed by

TABLE I. The intrinsic Schiff moment, in units of e fm^3 and the intrinsic-state expectation values of operators in Eq. (10), in units of 10^{-3} fm^{-4}.

	$\langle \hat{S}_z \rangle$	$\langle \boldsymbol{\sigma\tau} \cdot \boldsymbol{\nabla} \rho_0 \rangle$	$\langle \boldsymbol{\sigma\tau} \cdot \boldsymbol{\nabla} \rho_1 \rangle$	$\langle \boldsymbol{\sigma} \cdot \boldsymbol{J}_0 \rangle$	$\langle \boldsymbol{\sigma} \cdot \boldsymbol{J}_1 \rangle$	$\langle \boldsymbol{\sigma\tau} \cdot \boldsymbol{J}_0 \rangle$	$\langle \boldsymbol{\sigma\tau} \cdot \boldsymbol{J}_1 \rangle$
SIII(0)	34.6	-1.081	-0.087	-1.047	0.162	-1.049	0.159
SkM*(0)	46.6	-0.730	-0.497	-1.043	0.099	-1.042	0.085
SLy4(0)	43.4	-0.676	-0.578	-1.303	-0.016	-1.299	-0.019
SkO$'$(—)	41.7	-0.343	-0.318	-1.149	0.030	-1.149	0.030
SkO$'$	41.7	-0.467	-0.227	-0.476	0.014	-0.526	0.014
Reference [6]	24	-2	-0.4				

gauge invariance [39] (a generalization of Galilean invariance), appear in the T-odd parts of these forces.

We rely on the crudest forms of projection. For parity, that means none at all, and for angular momentum it means inserting the rigid-rotor factor $J/(J+1)=1/3$ in front of the intrinsic Schiff moment, as described above. In other words, we use Eq. (6) with the intrinsic state taken to be the Hartree-Fock ground state produced by HFODD. Just as in the particle-rotor model, the intrinsic Schiff moment is given by the classical expression, Eq. (1), but with ρ_{ch} equal to e times the Hartree-Fock ground-state proton density. As already mentioned, the Hartree-Fock approximation allows us, by summing over occupied orbits, to write the intrinsic matrix element of the two-body potential $\hat{V}_{PT}$ as the expectation value of an effective one-body operator $\hat{U}_{PT}$. Because we now have a microscopic version of the "core," this effective potential is more complicated than in Eq. (8), and it now acts on all the nucleons:

$$\hat{U}_{PT} = \frac{g}{2m_\pi^2 m_N} \sum_{i=1}^{A} \boldsymbol{\sigma}_i \tau_{z,i} \cdot \boldsymbol{\nabla} \int d^3 r' \left(\frac{m_\pi^2 e^{-m_\pi|r-r'|}}{4\pi|r-r'|} \right)$$

$$\times [(\bar{g}_0 + 2\bar{g}_2)\rho_1(r') - \bar{g}_1 \rho_0(r')] + \text{exchange}. \quad (9)$$

Here, $\rho_0(r) \equiv \rho_n(r) + \rho_p(r)$ and $\rho_1(r) \equiv \rho_n(r) - \rho_p(r)$ are the isoscalar and isovector densities. The part resulting from exchange terms in the original two-body interaction $\hat{V}_{PT}$ is nonlocal, just as in the usual Hartree-Fock mean field, and we have not written it explicitly here (though we do below).

The code HFODD at present cannot evaluate the expectation value of a folded potential like the one above, which is due to the finite pion range. Nevertheless, even in the zero-range approximation we can avoid several of the assumptions—proportionality of neutron and proton densities, negligibility of exchange terms, and absence of core spin—leading to the extremely simplified potential in Eq. (8). The zero-range approximation is equivalent to assuming that the pion is very heavy, so that the term involving the pion mass in Eq. (9) becomes a δ function. Under this assumption, but none other, the exchange terms become local and $\hat{U}_{PT}$ takes the form

$$\hat{U}_{PT}(r) \rightarrow -\frac{g}{2m_\pi^2 m_N} \left\{ \sum_{i=1}^{A} \boldsymbol{\sigma}_i \tau_{z,i} \cdot [(\bar{g}_0 + 2\bar{g}_2)\boldsymbol{\nabla}\rho_1(r) \right.$$

$$-\bar{g}_1 \boldsymbol{\nabla}\rho_0(r)] + \frac{1}{2} \sum_{i=1}^{A} \boldsymbol{\sigma}_i \cdot [(-3\bar{g}_0 + \bar{g}_1 \tau_{z,i})\boldsymbol{J}_0(r)$$

$$\left. + (\bar{g}_1 + \bar{g}_0 \tau_{z,i} - 4\bar{g}_2 \tau_{z,i})\boldsymbol{J}_1(r)] \right\}. \quad (10)$$

Here, $\boldsymbol{J}(r)$ is the "spin-orbit" current, defined, e.g., in Ref. [17], and references therein, and the subscripts 0 and 1 refer to isoscalar and isovector combinations as they do for the density. The terms in $\hat{U}_{PT}$ that contain $\boldsymbol{J}$ are the exchange terms omitted above. We will evaluate them, but argue later that their effects are probably small when the finite range is restored. The terms containing the density ρ all result from the direct part of $\hat{V}_{PT}$. We do not simplify things further to obtain something like Eq. (8), because ρ_p is not really proportional to ρ_n and the core nucleons do carry some spin. We will manage nevertheless, to compare our results with those of Ref. [6]. We will also estimate the effect of a finite pion range on the direct terms, though our inability to do so more precisely at present is the most significant shortcoming of this work.

HFODD works by diagonalizing the interaction in the eigenbasis of an optimal anisotropic three-dimensional harmonic oscillator. For ^{225}Ra, algorithms developed in Ref. [34] give oscillator frequencies of $\hbar\omega_z = 7.0625$ and $\hbar\omega_\perp = 8.6765$ MeV in the directions parallel and perpendicular to the elongation axis. The matrix element of $\hat{U}_{PT}$ converges only slowly as we increase the number of levels in the basis. When the interaction polarizes the core, it takes 2500 or more single-particle basis states to get convergence. The basis then contains up to $N_z = 26$ and $N_\perp = 21$ oscillator quanta.

B. Laboratory Schiff moment of ^{225}Ra

We turn finally to results in ^{225}Ra itself. For SkO$'$, our HFODD calculations yield $\beta_2 = 0.190$, $\beta_3 = 0.146$, and $\beta_4 = 0.136$ for the usual first-order approximation to the deformation parameters determined from mass multipole moments [29]. The laboratory Schiff moment, Eq. (6), is proportional to the product of the intrinsic Schiff moment $\langle \hat{S}_z \rangle$

and the expectation value $\langle \hat{V}_{PT} \rangle$. Table I shows the intrinsic moments and the expectation values of the six operators that enter the zero-range approximation to $\hat{V}_{PT}$ in Eq. (10). Before commenting on the entries, we mention what is in each of the forces and calculations.

For all the forces, terms in the functional that are proportional to Laplacians of spin densities ($s \cdot \Delta s$) and density-dependent spin-spin terms ($f(\rho)s \cdot s$), cf. Refs. [17,39] which enter through the T-odd part of the Skyrme functional, have been turned off. For the first three rows in Table I [forces labeled with (0)], the spin-spin terms have also been turned off, so that the only nonzero terms in the T-odd functional (as noted above) are those required by gauge invariance. For the fourth row [SkO$'$(—)], all T-odd terms in the functional have been turned off, so that aside from the self-consistency in the wave functions the calculation resembles one with a phenomenological (non-self-consistent) potential, for which T-odd mean fields are never considered. We include this result so that we can distinguish the role played by core polarization. The results in the line labeled SkO$'$ include the time-odd channels, adjusted as discussed above [17]. This is the force in which we have the most confidence. The last entry is the result of Ref. [6], with the implicit assumption that the neutron and proton densities are proportional.

In our calculations, the intrinsic Schiff moments are close to one another, and all are less than twice the estimate of Ref. [6]. The agreement reflects the collective nature of these intrinsic moments; they are even larger than the particle-rotor estimates. But the matrix elements of $\hat{V}_{PT}$, the other ingredient in Eq. (6) for the laboratory Schiff moment, are a bit more delicate. Our results show the exchange terms on the right side of the table to be comparable to the direct terms, a result that is surprising because for a spin-saturated core (or in the particle-rotor model) the exchange terms vanish exactly. We think, however, that the ratio of exchange to direct terms would become small, were the finite range of the interaction reintroduced and short-range NN correlations inserted.

Though unable to include either effect here, we did so in a Nilsson model for ^{225}Ra. We took nucleons there to occupy independent single-particle levels generated by a deformed oscillator potential with $\beta_2 = 0.138$, $\beta_3 = 0.104$, and $\beta_4 = 0.078$, values taken from Ref. [6]. We then evaluated the ground-state expectation value of the full two-body interaction $\hat{V}_{PT}$, with and without the zero-range approximation (and in the latter case, with short-range correlations included in the manner of Ref. [40]). In this simple model, the valence nucleon carries all the spin, and only the neutron-proton and neutron-neutron parts of $\hat{V}_{PT}$ contribute. The direct np term shrank by a factor of 1.5, while the corresponding exchange term shrank by a factor of 1400 [both independent of the $\bar{g}$'s in Eq. (4), it turns out] when the range of the interaction was set to its proper value. The results in the nn channel were less dramatic: the direct part again shrank by 1.5 and the exchange part by a factor of 5. When we moved the valence neutron to higher orbits, these numbers changed some—the direct terms sometimes were not suppressed at all and other times shrank by factors of up to 6, but the ratios of the

TABLE II. Intrinsic-state expectation values of important matrix elements, in the neutron-proton scheme, in units of 10^{-3} fm^{-4}.

	$\langle \boldsymbol{\sigma}_n \cdot \boldsymbol{\nabla} \rho_n \rangle$	$\langle \boldsymbol{\sigma}_n \cdot \boldsymbol{\nabla} \rho_p \rangle$
SIII(0)	−0.577	−0.491
SkM*(0)	−0.619	−0.120
SLy4(0)	−0.628	−0.050
SkO$'$(—)	−0.331	−0.013
SkO$'$	−0.320	−0.114
Reference [6]	−1.2	−0.8

exchange to direct contributions almost always ended up small. Similar behavior was found for parity-violating forces in Ref. [41], where it was traced in part to the different average momenta carried by the pion in direct and exchange graphs. So that we can compare our results with those of Ref. [6], we will neglect the exchange terms from now on, though we caution that this step should eventually be justified more rigorously, e.g., by actually calculating them with the finite-range force in the full mean-field model. The reduction we see in the direct terms is in line with the results of Ref. [42], though we find it more variable.[2]

Though we cannot yet be more quantitative about finite-range effects, we do quantify the core polarization in Table I. For the first three rows of the table, where the forces are labeled (0), the spin-spin terms are absent from the energy functional, and the protons in the core develop only a small spin density from the T-odd terms required by gauge invariance. For the fourth row, SkO$'$(—), all T-odd terms are absent and the protons can have no spin at all. This means that the operators $f(\boldsymbol{r})\boldsymbol{\sigma}$ and $f(\boldsymbol{r})\boldsymbol{\sigma}\tau$ have either the same or almost the same expectation value for any $f(\boldsymbol{r})$ so that columns 4 and 6 ($\langle \boldsymbol{\sigma} \cdot \boldsymbol{J}_0 \rangle$ and $\langle \boldsymbol{\sigma}\tau \cdot \boldsymbol{J}_0 \rangle$) have identical or nearly identical entries for these forces, and so do columns 5 and 7 ($\langle \boldsymbol{\sigma} \cdot \boldsymbol{J}_1 \rangle$ and $\langle \boldsymbol{\sigma}\tau \cdot \boldsymbol{J}_1 \rangle$). The fifth row of the table contains the effects of spin polarization, which are primarily to alter the neutron-spin density; the equalities between the columns are not badly broken, so the protons do not develop much spin. The same is true of the terms involving ρ, though that is not obvious from the table because we display only the two terms that appear in Eq. (10).

These near equalities and the probable irrelevance of the exchange terms when the finite range is taken into account imply that only the quantities $\boldsymbol{\sigma}_n \cdot \boldsymbol{\nabla} \rho_n$ and $\boldsymbol{\sigma}_n \cdot \boldsymbol{\nabla} \rho_p$ are ultimately important. We display them in Table II. Except for SIII, the neutron-density distribution affects the matrix element much more than that of protons. By comparing the fourth and fifth rows, however, we see that spin correlations increase the role of the protons, while reducing that of the neutrons slightly. Thus, while the spin-spin interactions do

---

[2]We performed another test, using the direct part of Eq. (10) with the valence wave function taken from the Nilsson model just described, but with the neutron and protons densities assumed to have more realistic Woods-Saxon forms. The direct terms were again suppressed by factors of 1.5 to almost 10 that depended significantly on the valence orbit.

not cause the protons to develop much net spin, they do correlate the neutron spin with the proton density.

There is not too much scatter in our results. The entries in the second column ($\langle \boldsymbol{\sigma}\tau\cdot\boldsymbol{\nabla}\rho_0\rangle$) of Table I differ by factors of 2 or 3, and the entries in the third ($\langle \boldsymbol{\sigma}\tau\cdot\boldsymbol{\nabla}\rho_1\rangle$) by a little more, though they are all smaller than those in the second column (which is not surprising—the third column subtracts the neutron and proton densities, while the second adds them). In the neutron-proton scheme (Table II) all of our numbers are smaller than those of Ref. [6], a result that was anticipated in Ref. [8]. The difference from the earlier estimate for the larger matrix elements ranges from factors of 2 to 4, though the isovector combination—the third column in Table I—is sometimes actually enhanced a little.

What, at last, have we to say about the real laboratory Schiff moment S? The lab moment is given by the product of the matrix elements just discussed, the intrinsic Schiff moments, and the unknown coefficients $\bar{g}_i$. Our intrinsic Schiff moments are about 1.5 times larger than those of Ref. [6], while our $\hat{V}_{PT}$ matrix elements, in the zero-range approximation, are smaller than theirs, usually by a somewhat larger amount. Overall, our lab moments will usually be smaller by factors between about 1.5 and 3 than the estimates of Ref. [6] (an exception can occur if for some reason $\bar{g}_1$ is considerably less than the other two coefficients).

How large are our moments compared to that of ^{199}Hg? The most comprehensive calculation in that nucleus, which appeared very recently [43], improved on the work of Ref. [44] by including the effects of the residual strong interaction and the full finite-range form for $\hat{V}_{PT}$. The new results are smaller than that of Ref. [44], only slightly so for the isovector part of $\hat{V}_{PT}$, but by a considerable amount in the isoscalar and isotensor channels. The authors write their results in terms of the pion-nucleon couplings as

$$S_{\text{Hg}} = 0.0004 g\bar{g}_0 + 0.055 g\bar{g}_1 + 0.009 g\bar{g}_2 \quad (e\ \text{fm}^3). \quad (11)$$

Our result for radium, with the zero-range approximation and exchange terms neglected, translates to

$$S_{\text{Ra}}^{\text{zero-range}} = -5.06 g\bar{g}_0 + 10.4 g\bar{g}_1 - 10.1 g\bar{g}_2 \quad (e\ \text{fm}^3). \quad (12)$$

If the three $\bar{g}$'s are comparable, our Schiff moment is several hundred times larger than that of Ref. [43], in part because the isoscalar and isotensor interactions are more effective in Ra than in Hg. (If $\bar{g}_1$ is larger than the other two couplings, as in left-right symmetric models [45], our result is less than 200 times bigger than the latest one in ^{199}Hg. The very small coefficient of $\bar{g}_0$ for ^{199}Hg in Eq. (11), by the way, has significant consequences [45] for the limit on the QCD T-violating parameter $\bar{\theta}$ that can be inferred from the experimental limit in Ref. [4].) Accepting the work of Ref. [46] on atomic physics in Ra and Hg, the enhancement of the atomic

EDM of ^{225}Ra is about three times that of the Schiff moment, i.e., potentially more than 1000. We again caution, however, that we have yet to include the full finite-range version of $\hat{V}_{PT}$, and that our preliminary investigations suggest that doing so will decrease our Schiff moment at least a little. Ironically, Ref. [43] finds that including the finite range actually increases the matrix element in ^{199}Hg, though only slightly.

We hope to make other improvements in our calculation as well. Projection onto states of good parity will change the results a bit, as will angular momentum projection. Our conclusions about the size of spin-polarization corrections could be modified by two terms in the Skyrme functional that we have set to zero, or by a better determined value of the Landau parameter g_0. Whatever the result of such corrections, however, it is clear that the atomic EDM of ^{225}Ra will always be significanlty larger than that of ^{199}Hg.

V. CONCLUSIONS

We have calculated the Schiff moment in ^{225}Ra in the approximation that the T-violating interaction has zero range. Our calculations, which are self-consistent and include core polarization, give results that are generally just a few times smaller than earlier estimates based on the particle-rotor model. Accepting the very recent results of Ref. [43], we currently find the Schiff moment of ^{225}Ra to be (generically) several hundred times that of ^{199}Hg, a result that strengthens the case for an atomic-EDM experiment in Ra, though the enhancement factor depends significantly on the source of T violation, and we expect it to decrease at least a little when we use the finite-range force. Work towards including a finite range in HFODD is in progress. We also plan to apply the self-consistent methods used here to other light actinides, as well as to ^{199}Hg, where we suspect octupole correlations may play some role [8]. Maintaining self-consistency in ^{199}Hg should automatically control the spurious Schiff strength encountered in Ref. [43]. The source of the insensitivity of the Schiff moment to T violation in the isoscalar channel in that work should be checked and understood.

After many years of neglect, the question of which isotopes are the best for EDM measurements is now being rapidly addressed.

[1] For a recent review, see, e.g., R.V. Kowalewski, hep-ex/0305024.

[2] R.G. Sachs, *The Physics of Time Reversal* (Chicago Press, Chicago, 1987).

[3] I.B. Khriplovich and S.K. Lamoreaux, *CP Violation Without Strangeness: Electric Dipole Moments of Particles, Atoms, and Molecules* (Springer-Verlag, Berlin, Heidelberg, 1997), and references therein.

[4] M.V. Romalis, W.C. Griffith, J.P. Jacobs, and E.N. Fortson, Phys. Rev. Lett. **86**, 2505 (2001).

[5] L.I. Schiff, Phys. Rev. **132**, 2194 (1963).

[6] V. Spevak, N. Auerbach, and V.V. Flambaum, Phys. Rev. C **56**, 1357 (1997).

[7] N. Auerbach, V.V. Flambaum, and V. Spevak, Phys. Rev. Lett. **76**, 4316 (1996).

[8] J. Engel, J.L. Friar, and A.C. Hayes, Phys. Rev. C **61**, 035502 (1999).

[9] T. Chupp (private communication).

[10] R. Holt, http://mocha.phys.washington.edu/x]int_talk/WorkShops/int_02_3/People/Holt_R/(2002).

[11] W.C. Haxton and E.M. Henley, Phys. Rev. Lett. **51**, 1937 (1983).

[12] P. Herczeg, Hyperfine Interact. **43**, 77 (1988).

[13] I.S. Towner and A.C. Hayes, Phys. Rev. C **49**, 2391 (1994).

[14] G.A. Leander and R.K. Sheline, Nucl. Phys. **A413**, 375 (1984).

[15] O.P. Sushkov, V.V. Flambaum, and I.B. Khriplovich, Zh. Eksp. Teor. Fiz. **87**, 1521 (1984) [Sov. Phys. JETP **60**, 873 (1984)].

[16] M. Bender, P.-H. Heenen, and P.-G. Reinhard, Rev. Mod. Phys. **75**, 121 (2003).

[17] M. Bender, J. Dobaczewski, J. Engel, and W. Nazarewicz, Phys. Rev. C **65**, 054322 (2002).

[18] P.-G. Reinhard, D.J. Dean, W. Nazarewicz, J. Dobaczewski, J.A. Maruhn, and M.R. Strayer, Phys. Rev. C **60**, 014316 (1999).

[19] M. Beiner, H. Flocard, N.V. Giai, and P. Quentin, Nucl. Phys. **A238**, 29 (1975).

[20] J. Bartel, P. Quentin, M. Brack, C. Guet, and H.B. Håkansson, Nucl. Phys. **A386**, 79 (1982).

[21] E. Chabanat, P. Bonche, P. Haensel, J. Meyer, and R. Schaeffer, Nucl. Phys. **A635**, 231 (1998); **A643**, 441(E) (1998).

[22] P.A. Butler and W. Nazarewicz, Rev. Mod. Phys. **68**, 349 (1996).

[23] E. Garrote, J.L. Egido, and L.M. Robledo, Phys. Lett. B **410**, 86 (1997).

[24] A. Tsvetkov, J. Kvasil, and R.G. Nazmitdinov, J. Phys. G **28**, 2187 (2002).

[25] M. Bender, Ph.D. thesis, Johann Wolfgang Goethe–Universität, Frankfurt am Main, 1998.

[26] M. Bender, K. Rutz, P.-G. Reinhard, and J.A. Maruhn, Eur. Phys. J. A **8**, 59 (2000).

[27] J.L. Egido and L.M. Robledo, Nucl. Phys. **A494**, 85 (1989).

[28] K. Rutz, J.A. Maruhn, P.-G. Reinhard, and W. Greiner, Nucl. Phys. **A590**, 680 (1995).

[29] P. Ring and P. Schuck, *The Nuclear Many-Body Problem* (Springer-Verlag, New York, 1980), Eq. 1.35.

[30] R.H. Spear, At. Data Nucl. Data Tables **42**, 55 (1989).

[31] S. Raman, C.W. Nestor, Jr., and P. Tikkanen, At. Data Nucl. Data Tables **78**, 1 (2001).

[32] G.E. Brown, in *Facets of Physics*, edited by D. Allan Bromley and Vernon W. Hughes (Academic Press, New York, 1970).

[33] J.P. Blaizot and G. Ripka, *Quantum Theory of Finite Sytems* (MIT Press, Cambridge, MA, 1986), p. 347, Problem 10.14.

[34] J. Dobaczewski and J. Dudek, Comput. Phys. Commun. **102**, 166 (1997); **102**, 183 (1997).

[35] J. Dobaczewski and J. Dudek, Comput. Phys. Commun. **131**, 164 (2000).

[36] P. Olbratowski, J. Dobaczewski, and J. Dudek, Comput. Phys. Commun. (to be submitted).

[37] F. Osterfeld, Rev. Mod. Phys. **64**, 491 (1992).

[38] W. Zuo, C. Shen, and U. Lombardo, Phys. Rev. C **67**, 037301 (2003).

[39] J. Dobaczewski and J. Dudek, Phys. Rev. C **52**, 1827 (1995); **55**, 3177(E) (1997).

[40] G.A. Miller and J.E. Spencer, Ann. Phys. **100**, 562 (1976).

[41] E.G. Adelberger and W.C. Haxton, Annu. Rev. Nucl. Part. Sci. **35**, 501 (1985).

[42] A. Griffiths and P. Vogel, Phys. Rev. C **44**, 1195 (1991).

[43] V.F. Dmitriev and R.A. Sen'kov, nucl-th/0304048.

[44] V.V. Flambaum, I.B. Khriplovich, and O.P. Sushkov, Nucl. Phys. **A449**, 750 (1986).

[45] P. Herczeg, in *Tests of Time Reversal Invariance in Neutron Physics*, edited by N.R. Rogerson, C.R. Gould, and J.D. Bowman (World Scientific, Singapore, New Jersey, Hong Kong, 1988), p. 24.

[46] V.A. Dzuba, V.V. Flambaum, J.S.M. Ginges, and M.G. Kozlov, Phys. Rev. A **66**, 012111 (2002).